Use of sulfuric acid-carbonization materials from grape pulp for the removal of hexavalent chromium (Cr(VI)): mechanism and characterization

Hasan Arslanoğlu & Harun Çiftçi

Taylor & Francis
Taylor & Francis Group

Check for updates

Use of sulfuric acid-carbonization materials from grape pulp for the removal of hexavalent chromium (Cr(VI)): mechanism and characterization

Hasan Arslanoğlu[a] (ID) and Harun Çiftçi[b] (ID)

[a]Department of Chemical and Process Engineering, Faculty of Engineering and Architecture, Kırşehir Ahi Evran University, Kırşehir, Turkey; [b]Department of Medical Biochemistry, Faculty of Medicine, Kırşehir Ahi Evran University, Kırşehir, Turkey

ABSTRACT

This study investigated the reduction of hexavalent chromium (Cr(VI)) with sulfur dioxide (SO_2) and adsorption of Cr(VI) onto dried grape pulp carbonized with sulfuric acid. Cr(VI) reduction capacities of SO_2 were determined. The filtrate was titrated with NaOH solution after shaking and filtering the carbonized material to retain unreacted sulfuric acid (H_2SO_4). Simple washing recovered 25–38% of the experimental acid at low concentrations. The carbonized material was washed twice with distilled water and then dried at 105 °C and weighed. The carbonized material had a yield of 56.6% (grape pulp/sulfuric acid ratios of 1:2), and the lower the H_2SO_4 content, the better the yield, suggesting that the higher the acid content, the lower the Cr(VI) content per unit grape pulp. Cr(VI) reduction capacities were 219.5, 195.3, and 190.9 mg Cr(VI)/g-H_2SO_4 for the grape pulp/sulfuric acid ratios of 1:1, 1:2, and 1:3, respectively.

Novelty statement: A carbonaceous material was obtained from grape pulp by carbonizing with concentrated sulfuric acid. The main objective of this study was to evaluate gas, liquid, and solid products or co-products obtained during carbonization process for hexavalent chromium treatment in aqueous solutions. In this context, (a) hexavalent chromium reduction capability of the gas evolved during carbonization was determined, (b) characterization of unreacted acid recovered by washing the carbonized product left after carbonization step was done, (c) carbonaceous adsorbent obtained was characterized and (d) hexavalent chromium adsorption characteristics of carbonaceous material obtained was determined.

HIGHLIGHTS

- Reduction and adsorption mechanisms of hexavalent chromium were investigated.
- A waste recycling method was proposed.
- The effects of sulfuric acid on carbonization were assessed.
- The structures and chemical compositions of a carbonized material were evaluated.
- The carbonized material is a cost-effective porous adsorbent for a clean environment.

Introduction

Chromium and its compounds are water contaminants. Therefore, their production and use for industrial purposes cause significant pollution. Chromium is found in aqueous media as cationic trivalent chromium (Cr(III)) and anionic hexavalent chromium (Cr(VI)) complex ions with different levels of toxicity (Huang *et al.* 2017; Wang *et al.* 2018, 2020). Moreover, a strong oxidizing Cr(VI) has mutagenic and carcinogenic effects. However, trivalent chromium is an essential element for animals up to a certain threshold and can be precipitated as hydroxide compound with much lower toxicity and more effectively than Cr (VI) (Förstner and Witmann 1983; Shakoori *et al.* 2000; Kobya 2004; Oğuz 2005).

The two stages of treatment are (1) reduction of Cr(VI) to Cr(III) and (2) precipitation and solid-liquid separation. The main substances used for Cr(VI) reduction in wastewater are sulfur dioxide (SO_2), alkali sulfite salts, and iron oxide (Fe (II)) salts (Sittig 1973; Patterson 1985). Studies on reverse osmosis, ion exchange, and adsorption have reported that a wide variety of inorganic and organic adsorbents can be used to remove Cr(VI) to Cr(III) by adsorption. Waste materials attract more attention than artificial ones because they result in a more cost-effective adsorption process (Arslanoglu and Tumen 2012; Wang *et al.* 2018; Yaras and Arslanoğlu 2018a, 2018b; Arslanoğlu 2019a; Wang *et al.* 2020).

Not only is Cr(VI) removed by adsorption into pectinized sugar beet pulp, but it is also partially reduced to Cr(III) (Özer *et al.* 1997). Research also shows that the

first carbonation mud (sugar factory waste) and its calcined materials are better at removing metal hydroxides from wastewater than alkalis (lime, sodium hydroxide, and sodium carbonate) (Kı yak *et al.* 1999; Güler *et al.* 2002).

Pectin is removed from the pulp by hot and long-term extraction with HCl solution (Özer *et al.* 1997). The solution phase in the small molecules in the pulp is removed together with the pectin. However, the depectinized sugar beet pulp is partially reduced to Cr(VI) (Özer *et al.* 1997), suggesting that pulp press water can also reduce Cr(VI) because it contains dissolved colloidal organic materials (Altundogan *et al.* 2004). Numerous studies use organic materials for Cr(VI) adsorption (Yurkow *et al.* 2002).

Carbon-based adsorbents are made of lignocellulosic agricultural and industrial waste. Some chemicals and methods are used to carbonize those substances, which are then used to adsorp pollutants (Arslanoğlu 2019a, 2019b). One of those methods involves sulfuric acid disrupting the structure of organic matter by absorbing water and converting it into carbon-containing materials (Namasivayam and Kadirvelu 1997; Namasivayam and Kadirvelu 1999; Selvi *et al.* 2001; Demirbaş *et al.* 2002; Kadirvelu *et al.* 2003; Kobya 2004; Huang *et al.* 2017; Wang *et al.* 2018, 2020).

Grapes are one of the world's largest fruit crops. Every year, 75 million tons of grapes are produced (Web 1), about 80% of which is used for wine production. Turkey is the sixth-largest grape producer, with more than 4 million tons per year as of 2018 (Web 2). However, only 2–3% is used for wine production (30 million liters of wine per year) (Web 3).

Grape pulp, also known as grape marc and grape pomace, is a winemaking by-product consisting of a grape stalk, grape peel, pulp, and kernels. Its composition depends on the type of grape and the wine production technique (Schieber *et al.* 2001).

About 20% of grapes are excreted as grape pulp during winemaking, resulting in nine million tons of grape pulp (25.000 tons in Turkey) every year. Unrecycled grape pulp accumulates and causes pollution.

The dried grape pulp is treated with concentrated sulfuric acid, and an SO_2-containing gas is released during the conversion of the active carbon-containing substance. Altundogan *et al.* (2007) found that the SO_2-containing gas effectively reduced Cr(VI) in aqueous solutions. Therefore, we investigated the Cr(VI) reduction capacity of the gas released during the carbonization of dried grape pulp by sulfuric acid. We also investigated the residual acid properties by washing with water, determined the yield of the carbonized material (CM), and conducted experiments on the CM to adsorb Cr(VI) from aqueous solutions.

Material method

Supply and preparation of grape pulp for experiments

The dried grape pulp was supplied from Elazig/Turkey. It was ground in an herb grinder and then sieved and divided into fractions of $-100 + 200$ mesh ($150\ \mu m < x < 75\ \mu m$) (Figure S1).

Cr(VI) stock solution

A Cr(VI) solution was prepared by dissolving potassium dichromate ($K_2Cr_2O_7$). A 2.83 g of $K_2Cr_2O_7$ (Riedel de Haen, 12,255) of 99% purity was weighed and added to a 1-L flask. Distilled water was added to dissolve $K_2Cr_2O_7$ to prepare a 1,000 mg/L Cr(VI) stock solution shaken to homogeneity.

Carbonization of grape pulp

An amount of 2 g of dried grape pulp was mixed with 96% H_2SO_4 (sulfuric acid). The grape pulp/sulfuric acid ratios were 1:1, 1:2, and 1:3 (CM1; CM2; CM3). The Erlenmeyer flask was heated in a heater (Heating continued at a temperature of 150 °C until the gassing ceased, this process took about an hour). The released gas was passed sequentially through 1,000 mg/L Cr(VI) solutions in washing bottles. The gas-solution reaction changed the color of the solution from orange to green. The reduction capacity of Cr(VI) in the solutions was determined. Figure 1 shows the experimental apparatus.

Recovery of residual acid from carbonization process and acid tests

Distilled water was ten times the weight of the starting solid. The carbonized material was shaken for 30 min with distilled water and then filtered (Blue tape filter paper, Double Rings-203). The acidity of the filtrate was determined using acidimetric titration.

Tests on carbonized material

The acid from the first wash was kept for testing. The carbonized material was rinsed twice with the same amount of water and then was filtered. The filters were discarded. The resulting solid was dried at 105 °C and then weighed. The yield of the carbonized material was calculated.

An amount of 2 g of carbonized grape pulp was shaken with a solution of Cr(VI) at a concentration of 100 mg/L at 200 rpm to determine its Cr(VI) adsorption property at different times (A kinetic study was performed by taking 2 mL of samples in 5, 10, 20, 30, 45, 60, 90, and 120 min).

Analysis

Cr(VI) analysis

Hexavalent chromium was spectrophotometrically analyzed using the diphenylcarbazide method (APHA 1975). The necessary reagents were prepared as follows: To prepare the diphenyl carbazide solution, 0.5 g of 1,5-diphenyl carbazide was dissolved in 100 mL of acetone. On the other hand, 6 N H_2SO_4 solution was prepared by taking 167 mL of the 96% H_2SO_4 solution and completing it to 1 L in a 1-L volumetric
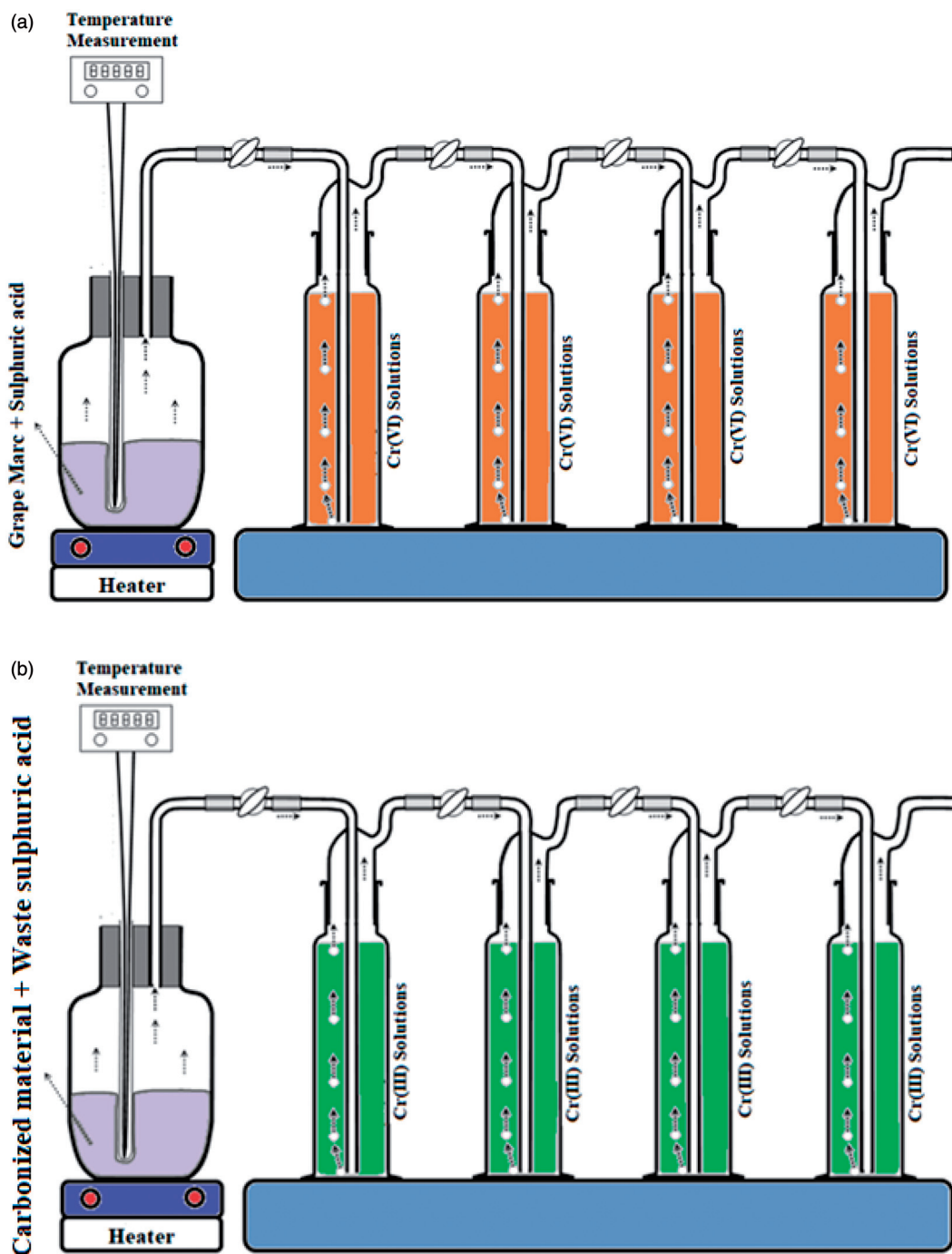
Figure 1. Cr(VI) reduction and carbonized material production system used in experiments, (a) Before Reduction, (b) After Reduction.

flask. Two milliliters of 6 N H_2SO_4 and 1 mL of diphenylcarbazide solution were placed in a 50-mL flask and then analyzed using a spectrophotometer (Shimadzu UV-1200) to compare the absorbance at 540 nm wavelength to standard values. The Cr(VI) content of the unknown sample was determined using a calibration graph of standard solutions (0.1–1.0 mg/L). The total Cr content in some samples was determined using an atomic absorption spectrometer (PerkinElmer AAnalyst 400). Flame was obtained using acetylene gas. For the analysis of total chromium, the standard calibration range was chosen between 1–5 mg/L. The absorbance values were used to calculate the corresponding concentrations. The removal rate of Cr(VI) from aqueous

solution by adsorption was calculated using Equation (1).

$$\text{Cr(VI) adsorption } \% = (C_o - C_s) \times \frac{100}{C_o} \qquad (1)$$

where C_0 and C_s (mg/L) are the initial and the equilibrium of aqueous Cr(VI) concentration, respectively.

After reaction, the adsorption capacity at equilibrium (q_e [mg/g]) was determined using Equation (2):

$$q_e = \frac{(C_0 - C_e)}{m} \times V \qquad (2)$$

where V (L) is the volume of the Cr(VI) solution; m (g) is the mass of the adsorbents; C_0 is the initial and the

equilibrium concentration of the Cr(VI) solution; C_e (mg/L) is the equilibrium concentration of the Cr(VI) solution.

Reduction and adsorption experiments were carried out in two parallel examples. When the results deviated at most 3% from each other, calculations were made by taking the average of two parallel experiments. A third experiment was performed in cases with few, but more deviations, and the average of two close experiments were taken into account.

Determination of acid

Concentrated sulfuric acid has such a strong affinity for water that it separates and removes many organic compounds into simple products. For this purpose, it is the residual amount of sulfuric acid used for carbonization after the process. A certain amount of sample (diluted if necessary) from the first wash was titrated with 0.1 N NaOH (F~1) using a phenolphthalein indicator until the solution turned pink. H_2SO_4 content obtained by washing from NaOH solution was calculated using Equation (3).

$$1 \text{ mL } 0.1 \text{ N NaOH solution} = 0.0049 \text{ g } H_2SO_4 \quad (3)$$

Instrumentation and measurements

The grape pulp and carbonization were characterized using a scanning electron microscopy-energy-dispersive x-ray spectroscopy (SEM-EDS) (FEI Quanta 250 FEG), ultimate analysis, and elemental analysis (LECO CHNS 932 Elemental Analyzer). Proximate analysis was carried out in a laboratory type electric oven according to ASTM standards to determine the moisture, ash, volatile matter, and fixed carbon contents. The Fourier transform infrared spectroscopy was used to identify functional groups on the carbon surface. FTIR analysis was performed with 4 cm^{-1} resolution in the 400–4,000 cm^{-1} scanning range. Measurements were made using the ATR mode. Specific surface area, total pore volume, and adsorption average pore diameter were calculated using the Brunauer−Emmett−Teller (BET, Micromeritics ASAP, 2020). Micropore volume, micropore area, and external surface area were determined with the t-plot method. The pore size distributions were determined via the nonlocal density functional theory (NLDFT) model. SEM micrographs were used to analyze adsorbent porosity and surface morphology before and after adsorption. FTIR spectra were used to document the important functional groups in the adsorbent. Thermal decomposition behavior of grape pulp pyrolysis was examined by thermal analyzer (FEI Quanta 250 FEG) under nitrogen gas atmosphere in the temperature range of 25–800 °C. The nitrogen flow rate was kept at 10 mL/min during the studied temperature range.

Results and discussion

Characterization of grape pulp

We presented the grape pulp properties before Cr(VI) reduction and removal. It will be useful to address the

Table 1. Chemical/physicochemical properties of grape pulp.

Properties	Value
Bulk density (g/cm^3)[a]	0.896
True density (g/cm^3)[b]	1.4974
Loss of heating at 105°C (humidity) (%)[c]	3.1
Loss of heating at 600°C (%)[d]	74.9
Ash (%)[e]	5.6
Potassium (%)[f]	1.74
Sodium (mg/kg)[f]	1,185
Calcium (mg/kg)[f]	3,500
Magnesium (mg/kg)[f]	810

[a]Weight of the grape pulp filled to a certain volume of container.
[b]Value found with helium pycnometer.
[c]Grape pulp dried at 80°C for 24h at 105°C.
[d]Grape pulp dried at 80°C, constant weighing result at 600°C.
[e]Grape pulp dried at 80°C with constant weighing at 950°C.
[f]By analysis of the solution obtained by dissolving the ash in 0.1 M HCl.

Table 2. Final and compositional analyses of grape pulp (Arslanoğlu, 2020a).

Component	Value (%)	Compositional analysis	Weight (%)
C	45.94±0.28	Hemi-cellulose	38.90±0.33
H	5.58±0.11	Cellulose	35.10±0.29
N	0.66±0.05	Lignin	17.70±0.71
S	0.09±0.02	Extractives	8.30
O	39.03±0.23	Calorific value (MJ/kg)	28.67

reduction and removal mechanisms. The characterization results of the grape pulp used in this study are given in Tables 1 and 2. Figure S2 shows the TGA-DTA analysis results. The grape pulp began to deteriorate significantly at 210 °C. The grape pulp lost weight at a specific rate up to about 450 °C. About 57.5% reduction in weight in that region was due to the removal of bound water and volatile organics. Weight dropped slightly between 450 and 700 °C, suggesting that the remainder of the organics was concentrated and that the carbonization started at the limit. The region lost about 8% of its weight, confirmed by SEM-EDX analysis on the grape pulp (Figure 2). The functional groups in the grape pulp and stabilized carbonized material (carbons) were analyzed. The figure shows the FTIR spectra of the grape pulp and the modified materials. The peak of 1,000–1,200 cm^{-1} (Yang and Lua 2003) in the fingerprint region indicates that the grape pulp skeleton contained cellulose. The peak, which characterizes free and esterified carboxyl at 1,650–1,750 cm^{-1}, may also indicate the presence of pectin (Al-Qodah and Shawabkah 2009). The 3,200–3,600 cm^{-1} region indicates hydroxyl groups in macromolecules (e.g., cellulose pectin) or water (Figure S3).

The FTIR spectral characteristics correspond to the tensile vibration of the free-hydroxide and H-bonded hydroxide of the broad-strong band of 3,200–3,600 cm^{-1}, mainly belonging to OH$^-$containing groups, such as water and alcohol. The absence of this band in carbonization materials suggests deterioration in the structure. The small peak in the pyrolysis material of the grape pulp at about 3,650 cm^{-1} can be attributed to the hydrogen bond of alcohol and phenol. It can be attributed to C-H vibration in the methyl and methylene groups peaked in the grape pulp surface and some pyrolysis materials at 2,900–3,000 cm^{-1} (Park et al. 1997) and C−H bending out of an aromatic plane. This was very small in the carbonized material. The peaks observed between 1,500 and 1,600 cm^{-1} may belong to C=C
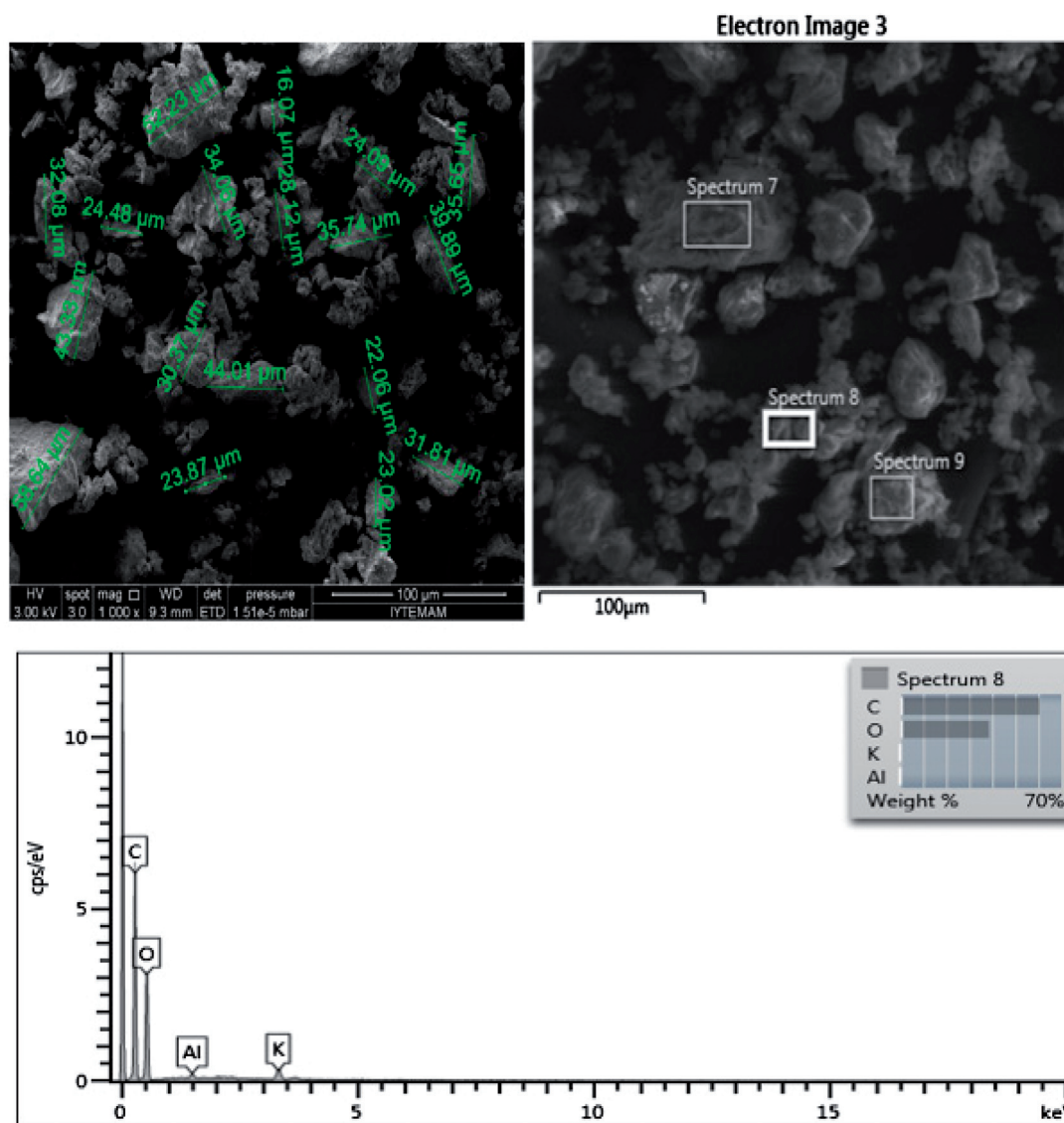
Figure 2. SEM image and EDX analysis of grape pulp.

stretching in aromatics. Besides, the peak observed at $1,600$ cm^{-1} in the spectrum of carbonized samples is likely to belong to the conjugated C=O strain vibration in the aromatic system frequently observed (Park *et al.* 1997). The peaks observed around 1,640 and 1,450 cm^{-1} may correspond to amide groups in carbons of starting materials with functional groups, such as an amine (Al-Qodah and Shawabkah 2009).

Characterization of carbonized material

SEM images allow us to observe the carbonized adsorbent pore and shape of particles before and after adsorption. Before adsorption, the SEM images indicated that the carbonized material had an irregular porous surface (Figure 3). After Cr(VI) adsorption, the empty spaces were filled (Figure 3). The EDS of the adsorbent before and after Cr(VI) adsorption (Figure 3(a,b)) shows the presence of Cr(VI) only after adsorption (Figure 3(b)), indicating that the adsorption was successful.

The spectrum of the adsorbent before Cr(VI) adsorption (Figure 4(a)) showed a broad peak at $3,414$ cm^{-1}, indicating the hydroxyl (-OH) and (-NH) groups. The C-H stretching of the alkyl groups gave a signal at $2,924.09$ cm^{-1}. The peak at $2,372.44$ cm^{-1} indicated the C≡N stretching or C≡C stretching. The characteristic peaks of the carbonyl (C=O) group at $1,735.93$ and $1,627.92$ cm^{-1} were also observed. The peak at $1,446.61$ cm^{-1} showed N-O stretch and O-H bending. Along with –OH and C=O groups, the peak at $1,319.31$ cm^{-1} showed the C-O stretch of the carboxylic (–COOH) group, whereas that at $1,244.09$ cm^{-1} indicated the C-H wag in the case of terminal alkyl halides. At $1,074.35$ cm^{-1}, the peak indicated the anhydride (CO–O–CO) stretching or C–O stretch and C-H bending. The peaks at 775.38 and 614.29 cm^{-1} indicated the C–Cl and C-Br stretch, respectively. After Cr(VI) adsorption (Figure 4(b)), the peak at $3,414$ cm^{-1} became less broad, and that at $1,627.92$ cm^{-1} became more intense and pointier, suggesting the involvement of O–H and N–H groups along with the C=O group. The reduction in the peaks at 1,319 and 775 cm^{-1} meant that the C-O and C–X binding
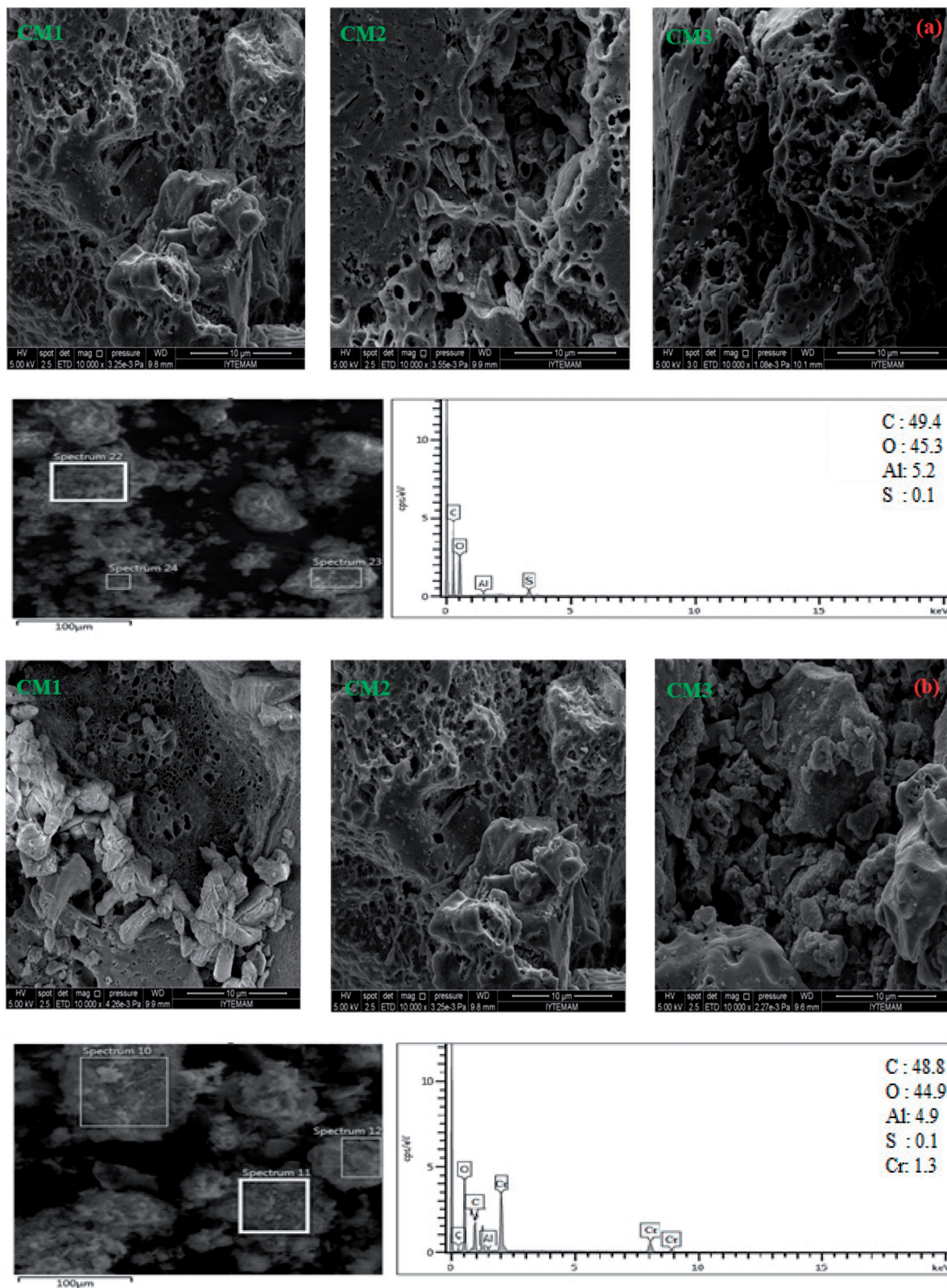
Figure 3. SEM-EDX images and evaluation of carbonized Material, (a) before adsorption, (b) after adsorption.

sites of the adsorbent were used entirely, resulting in an eventual reduction in signals. The carbohydrate and alkaloids were determined in the grape pulp (Park *et al.* 1997; Al-Qodah and Shawabkah 2009). Alkaloids (naturally occurring nitrogenous compounds) may contain sulfur, oxygen, phosphorous, chlorine, bromine, and nitrogen, carbon, and hydrogen. Hexavalent chromium is anionic at low pH (Fanning and Vannice 1993; Figueiredo *et al.* 1999). The nitrogen of alkaloids in the acidic medium became positively charged, suggesting that it may form a bond with anionic chromate because the spectra showed N–H, C–O, and C–X involvement.
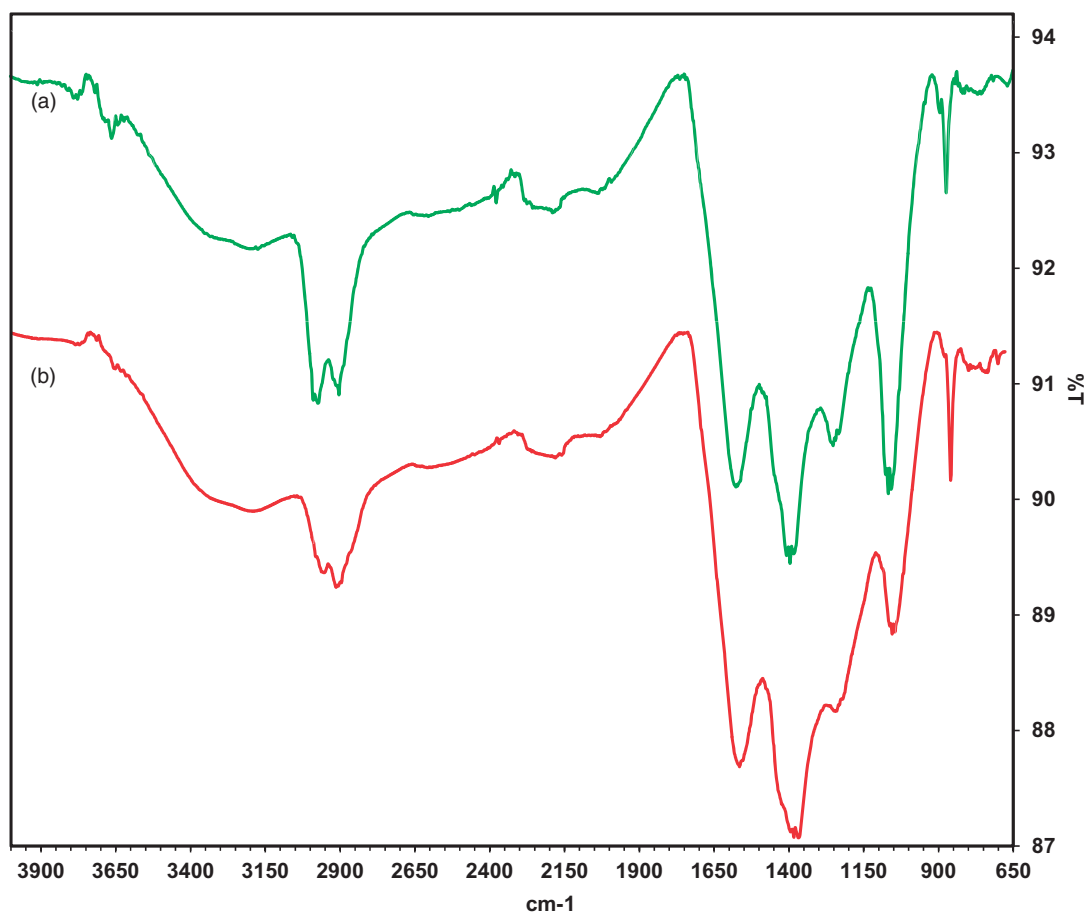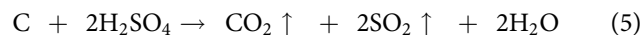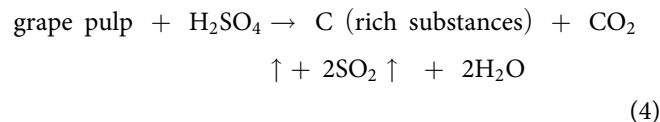
Figure 4. FTIR spectrum of carbonized material, (a) before adsorption, (b) after adsorption.

The BET model was used to measure the surface area and pore structure. CM3 had the largest BET surface area (514.662 m^2/g), total pore volume (0.584 cm^3/g), and adsorption average pore diameter (4.54 nm) (Table S1). Although CM2 had a lower surface area (421.88 m^2/g) and total pore volume (0.334 cm^3/g) than CM3, it had a higher adsorption average pore diameter (3.17 nm) than CM1. The results of experiments carried out to study the influence of impregnation ratio of grape pulp on the carbonized material features are presented in the table. Based on these results, it appears to play an extremely important role on the surface area and porosity of the carbonized materials. A raise in the BET surface area of activated carbon from 320.7 to 514.66 m^2/g throughout carbonization process was due to an increase in the impregnation ratio from 1 to 3. This may be explained by the development of microporosity of carbonized materials due to the gases in sulfuric acid and grape pulp structure serving as the precursor.

Carbonization yield

For carbonization at 150 °C, 2 g of grape pulp were mixed with sulfuric acid (96%) at ratios of 1:1, 1:2, and 1:3. The carbonization continued until no gas was released. The resulting carbonized material was washed three times in a row with 20-mL distilled water and then dried and weighed. Table S2 shows the yield of the carbonized material (Altundogan et al. 2007).

The higher the 96% H_2SO_4 content, the lower the carbonization (Table S2). Concentrated sulfuric acid draws water from organic substances and converts them into carbon (Equation (4)). It cannot occur altogether, but an increase in sulfuric acid content may result in a better reaction, accounting for the negative correlation between sulfuric acid content and the remaining mass. On the other hand, the carbon content after the first carbonization may partially reduce the unreacted sulfuric acid content (Equation (4)).

$$\text{grape pulp} + H_2SO_4 \rightarrow C \text{ (rich substances)} + CO_2$$
$$\uparrow + 2SO_2 \uparrow + 2H_2O$$
$$(4)$$

$$C + 2H_2SO_4 \rightarrow CO_2 \uparrow + 2SO_2 \uparrow + 2H_2O \quad (5)$$

This is also confirmed by the release of an SO_2-based gas during carbonization. The gas may increase the H_2SO_4 content and decrease the carbonized material content. As expected, the release of SO_2 may also be due to the oxidation of some functional groups (e.g., alcohol and aldehyde groups) that can be oxidized in organic matters (secondary alcohols will be oxidized to ketones. Primary alcohols will form aldehydes and carboxylic acids upon oxidation). For example, secondary alcohol groups in cellulose units are oxidized to form aldehyde, followed by carboxylic acid, while sulfuric acid can be partially reduced to SO_2 (Altundogan et al. 2007).

Table 3. Analyses and comments on acid recovery with washing.

|	H$_2$SO$_4$ (96%)/GP (g/g)		
	1.0	2.0	3.0
Grape pulp used in the experiments (g)	2	2	2
H$_2$SO$_4$ (96%) used in the experiments (g)	2	4	6
Pure H$_2$SO$_4$ (g) corresponding to 96% H$_2$SO$_4$ used in the experiments	1.92	3.84	5.76
Amount of water used in the first wash for acid recovery (mL)	20	20	20
Volume of 0.1 N NaOH solution consumed for 1 mL of acidic water (mL)	4.9	14.2	22.5
H$_2$SO$_4$ (g) obtained after washing	0.480	1.392	2.205
Ratio of acid recovered and acid used in reduction experiments (%)	25.00	36.25	38.28
Acid consumed in carbonization and subsequent heating (g)	1.440	2.448	3.555
SO$_2$ (g) corresponding to acid consumed in carbonization and subsequent heating	0.940	1.599	2.321
The amount of Cr (VI) that can theoretically be reduced by SO$_2$ according to Eckenfelder (*) (1,989) (mg)	508	864	1,255
Measured amount of reduced Cr(VI) (mg)	421	750	1,100
Experimental/theoretical amount of reduced Cr(VI) (%)	82.87	86.8	87.64

(*) According to Eckenfelder, 1.85 mg/L SO$_2$ is required to reduce Cr (VI) to 1 mg/L.

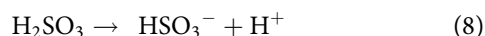## Cr(VI) reduction capacity of carbonization gases

The dried grape pulp (2 g) was mixed with sulfuric acid (96%) at ratios of 1:1, 1:2, and 1:3. The carbonization gas was passed through 125-mL K$_2$Cr$_2$O$_7$ solutions at 1,000 mg/L in each of the successive gas flasks (Figure 1). When the reduction at the first washing bottle was over, the bottle was deactivated, and a new one was connected to the back row. This process continued until no more gas was given off. After reduction, Cr(VI) reduction capacity in the grape pulp and sulfuric acid was evaluated (Table 3). Figure S4 shows the amount of grape pulp or sulfuric acid during reduction. The higher acid content resulted in higher Cr(VI) reduction per unit of pulp but lower Cr(VI) reduction per unit of H$_2$SO$_4$. Taking it as a constant, the reduction may be associated with the amount of sulfuric acid. This is the primary role of SO$_2$, resulting from the degradation of sulfuric acid during reduction (Altundogan et al. 2007).

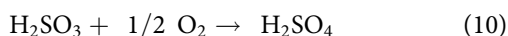## Recovery of residual acid remaining from Cr(VI) reduction

Sulfur dioxide (SO$_2$) first forms sulfurous acid (H$_2$SO$_3$) during carbonization (Equations (6 and 7)):

$$Cr_2O_7^{2-} + 3SO_2 + 2H_3O^+ \rightarrow 2Cr^{3+} + 3SO_4^{2-} + 3H_2O \tag{6}$$

$$SO_2 + H_2O \rightarrow H_2SO_3 \tag{7}$$
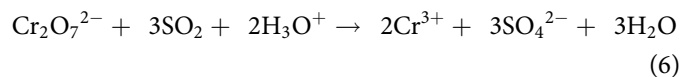
Sulfurous acid is ionized based on its masses (Equations (8 and 9)).

$$H_2SO_3 \rightarrow HSO_3^- + H^+ \tag{8}$$

$$\frac{[H] \times [HSO_3]}{[H_2SO_3]} = 1.72 \times 10^{-3} \tag{9}$$

$$H_2SO_3 + 1/2 \ O_2 \rightarrow H_2SO_4 \tag{10}$$

Only 1% of hydrogen sulfide with a pH >4.0 was H$_2$SO$_3$, and the reduction was slow, depending mainly on pH and temperature. At pHs <2, the reaction occurred very suddenly, and the amount of reagent needed was as high as the theoretical values (Eckenfelder 1989).

In theory, 1.85 mg/L of SO$_2$ is required for 1 mg/L of Cr(VI), and oxygen dissolved in a medium requires excess SO$_2$ due to the reaction of the active sulfide (Equation (9)) (Eckenfelder 1989).

The grape pulp/sulfuric acid ratios were 1:1, 1:2, and 1:3 during washing performed to recover the residual acid. The amount of acid was determined using titration with 0.1 N NaOH solution. Afterward, the recycled acid and the acid transformed into SO$_2$ were calculated (Table 3).

In general, H$_2$SO$_4$ degraded during carbonization turns into SO$_2$, which can reduce Cr(VI). The remaining H$_2$SO$_4$ can be obtained by washing. Almost half (35–49%) of the acid used in the experiments (grape pulp/sulfuric acid ratios of 1:1, 1:2, and 1:3) can be recovered as dilute acid with a simple wash (Table S3).

In the experiments, the acid converted to SO$_2$ during the carbonization was about 70, 71, and 73% of the theoretical values, respectively. They were not 100%, probably due to the decomposition of SO$_3$, the sulfone and sulfate groups in the solid matter, and SO$_2$ consumed by the dissolved oxygen, and gas leaks (Altundogan et al. 2007).

Cr(VI) adsorption of carbonized material

The carbonized material was shaken with a 100-mL solution at a concentration of 100 mg/L Cr(VI) at a constant temperature (25 °C) to determine the characteristic of Cr(VI) adsorption of the carbonized material. Table S4 shows the variation in pH (Initial pH = 3.45), while Figures S5 and S6 show the time-dependent Cr(VI) removal yield and Cr(VI) removal capacity (Arslanoğlu, Kaya, et al. 2020).

The carbonized material still had some acidity, although it was washed three times (Table S4). The acidity was higher, depending on the amount of acid in the carbonization, indicated by the low pH. The carbonized material can be washed with a light soda after the first wash to recover the residual acid. In some studies, materials carbonized with sulfuric acid are neutralized by contacting them with a sodium bicarbonate solution for a long time. However, if a material is to be used to remove anionic (chromate,

bichromate, and dichromate) materials, such as Cr(VI), it should be kept in mind that neutralization reduces the effectiveness of the adsorbent. Therefore, this study did not perform neutralization (Arslanoglu et al. 2008, 2009).

Figures S4 and S5 show that Cr(VI) adsorption onto the carbonized material is completed in the first 45 min. Both Table S4 and Figure S6 show that the more acidic the medium, the more effective the adsorption. The results also indicate that more sulfuric acid results in more effective material. However, increasing the amount of sulfuric acid does not have a significant effect. Considering the cost of sulfuric acid, we can state that the grape pulp/sulfuric acid ratio for activation is 1:1, suggesting that one gram of carbonized material removes about one gram of Cr(VI) in the first 15–30 min under experimental conditions.

Cr(VI) adsorption kinetics

The adsorption kinetics is of practical value because it can evaluate the yield of adsorption and scale-up operations (Arslanoglu 2019b). Therefore, the experimental data were modeled using the Lagergren pseudo-first- and second-order models (Equations (11) and (12)) to investigate Cr(VI) kinetics on CM1, CM2, and CM3. The Lagergren pseudo-first-order model (Lagergren 1898) for heterogeneous solid-liquid systems is formulated as follows:

$$q_t = q_e\left(1 - \exp^{-k_1 t}\right) \tag{11}$$

where q_e and q_t (mg/g) are the numbers of metal ions adsorbed at equilibrium and time t (min), respectively, under initial conditions $q_t = 0$ at $t = 0$. The slope obtained by plotting $\ln(q_e - q_t)$ versus time (min) (Figure S7(a)) allows us to estimate the constant rate of k_1 (min^{-1}).

The pseudo-second-order model (Ho and McKay 1999) allows us to calculate the reaction rate k_2 (g mg^{-1}min^{-1}), as follows:

$$q_t = \frac{q_e^2 k_2 t}{1 + q_e^2 k_2 t} \tag{12}$$

By plotting the experimental data t/q versus t, q_e, and k_2 were assessed from the slope and intercept, respectively (Table S5).

The pseudo-second-order equation is better at describing the adsorption process of the entire metal ions than the pseudo-first-order model. However, the pseudo-first-order model describes the first 45–60 min of adsorption better than the pseudo-second-order. Moreover, equation (12) considers adsorbent–adsorbate interaction and shows whether chemisorption occurs or not (Arslanoğlu 2019a; Eren et al. 2020).

Table S5 shows the kinetic parameters and correlation coefficients (R^2) for each model. Figure S7 (a) and (b) show the pseudo-first and -second-order plots, respectively. The relatively low R^2 values and the significant gap between the calculated and experimental adsorption capacity values suggested that the pseudo-first-order model did not fit the

adsorption of CM1, CM2, and CM3. The R^2 values for the pseudo-second-order model (0.9999, 0.9999, and 0.9997 for CM1, CM2, and CM3, respectively) were relatively higher than those of the pseudo-first-order model (0.9504, 0.9308, and 0.9409 for CM1, CM2, and CM3, respectively) (Arslanoglu 2017). The experimental q_e values agreed well with the calculated values. These results indicate that the adsorption of Cr(VI) onto CM1, CM2, and CM3 followed the pseudo-second-order model.

Cr(VI) adsorption isotherm

Adsorption isotherms are used to account for the relationship between liquid Cr(VI) and adsorbents at constant temperatures (Yaraş and Arslanoğlu 2019). In this study, the adsorption data agreed well with the Langmuir isotherm model and the Freundlich isotherm model in a non-linear form (Equations (13 and 14)). One of the most important isotherm adsorption models used to obtain information on adsorbate/adsorbent interaction is described by the Langmuir model Equation (13) (Langmuir 1918):

$$q_e = \frac{q_m K C_e}{1 + K C_e} \tag{13}$$

where q_e (mg g^{-1}) is the number of metal ions adsorbed per unit weight of adsorbate, C_e (mg L^{-1}) is the metal concentration at the equilibrium, K (L mg^{-1}) is the constant associated with adsorption heat.

According to Freundlich, the regions suitable for adsorption on the surface of an adsorbent are heterogeneous. In other words, they consist of different types of adsorption regions. The Freundlich isotherm (1907) for adsorption in a solution medium is as follows:

$$q_e = K_f C_e^{1/n} \tag{14}$$

Equation (14) is the Freundlich constant (mg g^{-1}), a measure of K_f: adsorption capacity, while the other Freundlich constant n is dimensionless.

Table S6 shows the isotherm parameters and correlation coefficients (R^2) for each model. Figure S8 shows the plot of the Langmuir and Freundlich isotherm models. Table S6 also shows that the R^2 values for the Langmuir isotherm model (0.9977, 0.9989, and 0.9959 for CM1, CM2, and CM3, respectively) were relatively higher than those for the Freundlich isotherm model (0.9321, 0.9457, and 0.9698 for CM1, CM2, and CM3, respectively), suggesting that the experimental data fit the Langmuir isotherm model better than the Freundlich isotherm model. In adsorption processes that conform to the Langmuir isotherm, the isotherm shape can also be evaluated according to a dimensionless R_L separation factor. From Equation (15), the value of R_L can be calculated. The R_L of CM1, CM2, and CM3 ranged from $0.158 \sim 0.356$, suggesting that Cr(VI) adsorption onto CM1, CM2, and CM3 was favorable under the given experimental conditions. The estimated maximum adsorption capacities of CM1, CM2, and CM3 were 12.12, 15.19, and 18.72 mg/g, respectively, which were relatively large in comparison to

other raw leaf materials, such as Onopordum Heteracantha (37.23 mg/g) (Ghorbani-Khosrowshahi and Behnajady 2016), magnetic carbon (44.72 mg/g) (Shang et al. 2016), carbonized materials (82.23 mg/g) (Zhou et al. 2016), and fallen coconut leaves (114.82 mg/g) (Sanna et al. 2016). In conclusion, the Langmuir isotherm model confirmed that Cr(VI) adsorption onto CM1, CM2, and CM3 was monolayer with similar affinities and activation energy over the homogeneous surface. The adsorption capacity of untreated grape pulp was found to be 3.45 mg/g under the same conditions. With this result, the effect of the carbonization process was seen actively.

$$r = 1/(1 + bC_0) \tag{15}$$

Numerous adsorption studies on Cr(VI) removal have obtained operating parameters (Langmuir constant, qmax) related to both kinetics and equilibrium (Table S7). It is seen that the carbonized material used in this study is not very good in removing Cr (VI) from aqueous solutions when compared to the literature in Table S7.

Thermodynamic studies

Thermodynamic parameters can also be calculated from the Langmuir constant. In this expression, when the C_e against C_e/q_e is plotted, the q and b values can be calculated from the slope and shift of the line, respectively. The thermodynamic parameters of the adsorption process such as free energy ($\Delta G°$), enthalpy ($\Delta H°$), and entropy ($\Delta S°$) can be calculated as explained below and with the equations below. The energy parameter of adsorption, b, has the following relationship with the adsorption enthalpy (Equation (16)). Thermodynamic parameters can be calculated using the Langmuir constant b. Thermodynamic parameters, including the Gibbs energy change ($\Delta G°$), the enthalpy change ($\Delta H°$), and the entropy change ($\Delta S°$), were calculated using Equations (16–18) (Arslanoglu 2019b; Arslanoğlu, Orhan, et al. 2020).

$$\ln b = \ln b_0 - \frac{\Delta H°}{RT} \tag{16}$$

$$\ln\left(\frac{1}{b}\right) = \frac{\Delta G°}{RT} \tag{17}$$

$$\Delta S° = (\Delta H° - \Delta G°)/RT \tag{18}$$

$\Delta G°$ is the free energy change (kJ mol^{-1}), T is the absolute temperature (K), R is the universal gas constant (8.314 Jmol^{-1}K^{-1}), $\Delta H°$ (kJ mol^{-1}) is the enthalpy change, and $\Delta S°$ (kJ mol^{-1}K^{-1}) is a function of entropy change T.

$\Delta G°$ plays a crucial role in the spontaneity of adsorption. The $\Delta G°$ values for CM1, CM2, and CM3 increased with an increase in temperature and were negative at all temperatures. These results indicated that the adsorption of CM1, CM2, and CM3 was favorable (Table S8). The $\Delta S°$ values for CM1, CM2, and CM3 were positive, suggesting increased interface entropy during adsorption. The positive $\Delta S°$ values

can be explained as follows: More than one water molecules displace one adsorbate molecule during chromium adsorption, increasing entropy (Arslanoglu 2019b). The $\Delta H°$ values for CM1, CM2, and CM3 were positive, meaning that the adsorption process was endothermic.

Conclusion

The gas released during dried grape pulp carbonization (with H_2SO_4) reduced the Cr(VI) concentration in aqueous solutions. The unreacted part of H_2SO_4 was recovered. Cr(VI) adsorption onto the carbonized material was also investigated. The grape pulp was mixed with sulfuric acid. The grape pulp/sulfuric acid ratios were 1:1, 1:2, and 1:3. The grape pulp was then heated for about an hour at 150 °C. The amount of solid material dried at 105 °C after the recovery of the unreacted acid was 66.25, 56.60, and 45% at the grape pulp/sulfuric acid ratios of 1:1, 1:2, and 1:3, respectively. The gas released during carbonization was passed through Cr(VI) solutions at 1,000 mg/L Cr(VI). The reduction capacity was 219.5, 195.3, and 190.9 mg at the grape pulp/sulfuric acid ratios of 1:1, 1:2, and 1:3, respectively. The grape pulp was heated at 150 °C with sulfuric acid (96%) until the end of the gas release for carbonization. About 25, 36.25, and 38.28% of sulfuric acid were recovered in the first washing at the grape pulp/sulfuric acid ratios of 1:1, 1:2, and 1:3, respectively. The remainder of the sulfuric acid was degraded by forming SO_3, reduced to SO_2, or perhaps spent by sulfating the solid. About one gram of carbonized material adsorbs about one gram of Cr(VI) when in contact with a 100 mL solution of 100 mg/L Cr(VI). Based on the result,

1. An carbonized material can be obtained by carbonizing grape pulp with a concentrated sulfuric acid solution.
2. Simple washing can be performed to recover unreacted sulfuric acid.
3. SO_2 gas resulting from decomposition can be used to reduce Cr(VI) in chromate solutions.

ORCID

Hasan Arslanoğlu 🔾 http://orcid.org/0000-0002-3132-4468
Harun Çiftçi 🔾 http://orcid.org/0000-0002-3210-5566

References

Al-Qodah Z, Shawabkah R. 2009. Production and characterization of granular activated carbon from activated sludge. Braz J Chem Eng. 26(1):127–136. doi:10.1590/S0104-66322009000100012.

Altundogan HS, Bahar N, Mujde B, Tumen F. 2007. The use of sulphuric acid-carbonization products of sugar beet pulp in Cr(VI) removal. J Hazard Mater. 144(1–2):255–264. doi:10.1016/j.jhazmat.2006.10.018.

Altundogan HS, Ozer A, Tümen F. 2004. A Study on the reduction of hexavalent chromium in aqueous solutions by vinasse. Environ Technol. 25(11):1257–1263. doi:10.1080/09593332508618368.

APHA. 1975. Stadart methods for examination of water and waste-water. 14th ed. Washington (DC): APHAWWA-WPCF; p. 192–194.

Arslanoğlu H, Altundogan HS, Tumen F. 2008. Preparation of cation exchanger from lemon and sorption of divalent heavy metals. Bioresour Technol. 99(7):2699–2705. doi:10.1016/j.biortech.2007.05.022.

Arslanoğlu H, Altundogan HS, Tumen F. 2009. Heavy metals binding properties of esterified lemon. J Hazard Mater. 164(2–3):1406–1413. doi:10.1016/j.jhazmat.2008.09.054.

Arslanoğlu H, Tumen F. 2012. A study on cations and color removal from thin sugar juice by modified sugar beet pulp. J Food Sci Technol. 49(3):319–327. doi:10.1007/s13197-011-0288-1.

Arslanoğlu H. 2017. Removal of Cu (II) from aqueous solutions by using marble waste. Pamukkale Uni J Eng Sci. 23(7):877–886. doi: 10.5505/pajes.2016.75688.

Arslanoğlu H. 2019a. Direct and facile synthesis of highly porous low cost carbon from potassium-rich wine stone and their application for high-performance removal. J Hazard Mater. 374:238–247. doi:10.1016/j.jhazmat.2019.04.042.

Arslanoğlu H. 2019b. Adsorption of micronutrient metal ion onto stru-vite to prepare slow release multielement fertilizer: copper (II) doped-struvite. Chemosphere. 217:393–401. doi:10.1016/j.chemosphere.2018.10.207

Arslanoğlu H, Kaya S, Tümen F. 2020. Cr(VI) adsorption on low-cost activated carbon developed from grape marc-vinasse mixture. Part Sci Technol. 38(6):768–781. doi:10.1080/02726351.2019.1632399.

Arslanoğlu H, Orhan R, Turan MD. 2020. Application of response surface methodology for the optimization of copper removal from aqueous solution by activated carbon prepared using waste polyurethane. Anal Lett. 53(9):1343–1365. doi:10.1080/00032719.2019.1705849.

Demirbaş E, Kobya M, Öncel S, Şencan S. 2002. Removal of Ni(II) from aqueous solution by adsorption onto hazelnut shell activated carbon: equilibrium studies. Bioresource Technol. 84:291–293. doi:10.1016/S0960-8524(02)00052-4.

Eckenfelder WW. 1989. Industrial water pollution control. 2nd ed. New York (NY): McGraw Hill; p. 98–103.

Eren MŞ, Arslanoğlu H, Çiftçi H. 2020. Production of microporous Cu-doped BTC (Cu-BTC) metal-organic framework composite materials, superior adsorbents for the removal of methylene blue (Basic Blue 9). J Environ Chem Eng. 8(5):104247. doi:10.1016/j.jece.2020.104247.

Fanning PE, Vannice MA. 1993. A Drifts study of the formation of surface groups on carbon by oxidation. Carbon. 31(5):721–730. doi:10.1016/0008-6223(93)90009-Y.

Figueiredo JL, Pereira MFR, Freitas MMA, Orfao JJM. 1999. Modification of the surface chemistry of activated carbons. Carbon. 37(9):1379–1389. doi:10.1016/S0008-6223(98)00333-9.

Förstner U, Wittmann GTW. 1983. Metal pollution in the aquatic environment. Berlin (Germany): Springer-Verlag.

Freundlich H. 1907. Über die adsorption in lösungen. Z Phys Chem. 57:385–470. doi:10.1515/zpch-1907-5723.

Ghorbani-Khosrowshahi S, Behnajady MA. 2016. Chromium(VI) adsorption from aqueous solution by prepared biochar from Onopordom Heteracanthom. Int J Environ Sci Technol. 13(7):1803–1814. doi:10.1007/s13762-016-0978-3.

Güler O, Gür F, Özer A, Tümen F. 2002. A study on the removal of heavy metals by carbonatation cake discarded in sugar industry. Int Sugar J. 104:458–462.

Ho YS, McKay G. 1999. Pseudo-second order model for sorption processes. Process Biochem. 34(5):451–465. doi:10.1016/S0032-9592(98)00112-5.

Huang W, Liu N, Zhang X, Wu M, Tang L. 2017. Metal organic frame-work g-C3N4/MIL-53 (Fe) heterojunctions with enhanced photo-catalytic activity for Cr (VI) reduction under visible light. Appl Surf Sci. 425:107–116. doi:10.1016/j.apsusc.2017.07.050.

Kadirvelu K, Kavipriya M, Karthika C, Radhika M, Vennilamani N, Pattabhi S. 2003. Utilazation of various agricultural wastes for acti-vated carbon preparation and application for the removal of dyes and metal ions from aqueous solutions. Bioresource Technol. 87(1):129–132. doi:10.1016/S0960-8524(02)00201-8.

Kıyak B, Özer A, Altundoğan HS, Erdem M, Tümen F. 1999. Cr(VI) Reduction in aqeous solutions by using copper smelter slag. Waste Manage. 19(5):333–338. doi:10.1016/S0956-053X(99)00141-5.

Kobya M. 2004. Removal of Cr(VI) from aqueous solutions by adsorption onto hazelnut shell activated carbon: kinetic and equilibrium studies. Bioresour Technol. 91(3):317–321. doi:10.1016/j.biortech.2003.07.001.

Lagergren S. 1898. Zur theorie der sogenannten adsorption geloster stoffe. Kungliga svenska vetenskapsakademiens. Handlingar. 24:1–39.

Langmuir I. 1918. The adsorption of gases on plane surfaces of glass, mica and platinum. J Am Chem Soc. 40(9):1361–1403. doi:10.1021/ja02242a004.

Namasivayam C, Kadirvelu K. 1997. Agricultural solid wastes for the removal of heavy metals: adsorption of Cu(II) by coirpith carbon. Chemosphere. 34(2):377–399. doi:10.1016/S0045-6535(96)00384-0.

Namasivayam C, Kadirvelu K. 1999. Uptake of mercury (II) from wastewater by activated carbon from an unwanted agricultural solid by-material: coirpith. Carbon. 37(1):79–84. doi:10.1016/S0008-6223(98)00189-4.

Oğuz E. 2005. Adsorption characteristics and the kinetics of the Cr(VI) on the Thuja oriantalis. Colloids Surf A. 252:121–128. doi:10.1016/j.colsurfa.2004.10.004.

Özer A, Tümen F, Bildik M. 1997. Cr(III) removal from aqueous solu-tions by depectinated sugar beet pulp. Environ Technol. 18(9):893–901. doi:10.1080/09593331808616608.

Park SH, McClain S, Tian ZR, Suib SL, Karwacki C. 1997. Surface and bulk measurements of metals deposited on activated carbon. Chem Mater. 9(1):176–183. doi:10.1021/cm9602712.

Patterson JW. 1985. Wastewater treatment technology. 2nd ed. Stoneham (MA): Butterworths Publisher.

Sanna H, Amit B, Eveliina R. 2016. Calcium hydroxyapatite microfi-brillated cellulose composite as a potential adsorbent for theremoval of Cr(VI) from aqueous solution. Chem Eng J. 283:445–452. doi:10.1016/j.cej.2015.07.035.

Schieber A, Stintzing FC, Carle R. 2001. By-materials of plant food processing as a source of functional compounds-recent develop-ments. Trends Food Sci Technol. 12(11):401–413. doi:10.1016/S0924-2244(02)00012-2.

Selvi K, Pattabhi S, Kadirvelu K. 2001. Removal of Cr(VI) from aque-ous sollution by adsorption on to activated carbon. Bioresource Technol. 80(1):87–89. doi:10.1016/S0960-8524(01)00068-2.

Shakoori AR, Makhdoom M, Haq RU. 2000. Hexavalent chromium reduction by a dichromate-resistant gram-positive bacterium isolated from effluents of tanneries. Appl Microbiol Biotechnol. 53(3):348–351. doi: 10.1007/s002530050033.

Shang J, Pi J, Zong M, Wang Y, Li W, Liao Q. 2016. Chromium removal using magnetic biochar derived from herb-residue. J Taiwan Inst Chem. Eng. 68:289–294. doi:10.1016/j.jtice.2016.09.012.

Sittig M. 1973. Pollutant removal handbook. Park Ridge (NJ): Noyes Data Corp.

Wang Y, Du B, Wang J, Wang Y, Gu H, Zhang X. 2018. Synthesis and characterization of a high capacity ionic modified hydrogel adsorb-ent and its application in the removal of Cr (VI) from aqueous solu-tion. J Environ Chem Eng. 6(6):6881–6890. doi:10.1016/j.jece.2018.10.048.

Wang Y, Yu L, Wang R, Wang Y, Zhang X. 2020. A novel cellulose hydrogel coating with nanoscale Fe0 for Cr (VI) adsorption and reduction. Sci Total Environ. 726:138625. doi:10.1016/j.scitotenv.2020.138625.

Web 1. Faostat. [accessed 2020 Apr 4]. http://faostat.fao.org/.

Web 2. [accessed 2020 Apr 4]. http://www.mapsofworld.com/world-top-ten/maps/world-top-ten-grape-producing-countries-map.jpg.

Web 3. Faostat. [accessed 2020 Apr 4]. http://faostat3.fao.org/browse/Q/QD/E.

Yang T, Lua AC. 2003. Characteristics of activated carbons prepared from pistachio-nut shells by physical activation. J Colloid Interface Sci. 267(2):408–417. doi:10.1016/S0021-9797(03)00689-1.

Yaras A, Arslanoğlu H. 2018a. Valorization of paper mill sludge as adsorbent in adsorption process of copper (II) ion from synthetic

solution: kinetic, isotherm and thermodynamic studies. Arab J Sci Eng. 43(5):2393–2402. doi:10.1007/s13369-017-2817-3.

Yaraş A, Arslanoğlu H. 2018b. Efficient removal of basic yellow 51 dye via carbonized paper mill sludge using sulfuric acid. Sigma J Eng Natural Sci. 36(3):803–818.

Yaraş A, Arslanoğlu H. 2019. Utilization of paper mill sludge for removal of cationic textile dyes from aqueous solutions. Sep Sci Technol. 54(16):2555–2566. doi:10.1080/01496395.2018.1552295.

Yurkow EJ, Hong J, Min S, Wang S. 2002. Photochemical reduction of hexavalent chromium (VI) in glycerol-containing solutions. Environ Pollut. 117(1):1–3. doi:10.1016/S0269-7491(01)00297-4.

Zhou L, Liu Y, Liu S, Yin Y, Zeng G, Tan X, Hu X, Hu X, Jiang L, Ding Y, et al. 2016. Investigation of the adsorption-reduction mechanisms of hexavalent chromium by ramie biochars of different pyrolytic temperatures. Bioresour Technol. 218:351–359. doi:10.1016/j.biortech.2016.06.102.